P9R.9 **ON THE DIFFERENTIAL PHASE IN THE MELTING LAYER**

A.V. Melnikov [(1)], **V. M. Melnikov** [(2)], and **A. V. Ryzhkov** [(2)]

[(1)] - *University of Oklahoma, Department of Computer Science, Norman, OK*
[(2)] - *Cooperative Institute for Mesoscale Meteorological Studies, University of Oklahoma, Norman, OK.*

1. Introduction

The cloud region where snowflakes melt is called the melting layer (or the bright band in radar meteorology). Processes in the melting layer form the size distribution of raindrops inside and below the layer. Polarimetric radars are unique tools for studying such processes. Differential reflectivity ZDR, and the linear depolarization ratio LDR, and cross-correlation coefficient ρ_{hv} in the melting layer have been in the focus of such studies for a long time (e.g., Doviak and Zrnic 1993, D'Amico et al. 1998, Russchenberg and Ligthart 1996, Bringi and Chandrasekar 2001). The behavior of another polarimetric variable, differential phase Φ_{DP}, was not well understood because of its strong oscillations within the melting layer.

Measured radar differential phase is a sum of the differential phase upon propagation and backscattering. It is considered that at S band, appreciable backscatter differential phase, δ, can be observed only in hail (e.g., Balakrishnan and Zrnic 1990, Doviak and Zrnic 1993). This is a manifestation of resonance effects that take place only for particles with sizes larger than 20 mm. For other hydrometeors, backscatter differential phase at S band is less than 1.5°, i.e., small, because of small imaginary part of dielectric permittivity of ice (snowflakes) or small oblateness of raindrops. Zrnic et al. 1993 demonstrated one more resonance effect: for oblate water drops with diameters from 10 to 15 mm, δ can exceed 10°. We consider this effect in the next section.

Ryzhkov and Zrnic (1998) showed that intrinsic differential phase can be biased in the presence of large gradients of radar reflectivity Z and Φ_{DP} within the radar resolution volume. This effect of nonuniform beam filling should be taken into account in the melting layer because of strong vertical gradients there.

Radar data collected with the polarimetric WSR-88D KOUN radar (Norman, OK) reveal a positive "bump" of the differential phase in the melting layer. In this paper, we examine such data and discuss their possible interpretation using different mechanisms including resonance scattering, nonuniform beam filling, and the new one that is described in section 4.

2. Radar data

We have analyzed radar data collected with KOUN in February and March 2005 in stratiform precipitation in central Oklahoma. Fig.1 displays PPI fields of Z_{DR} and Φ_{DP} on February 12, 2005 at elevation 2.7°. The corresponding radar reflectivity varied between 20 and 30 dBZ (not shown). In the differential reflectivity field, one can see a well pronounced ring of enhanced ZDR at the distances of about 50 km. The ZDR melting layer signature is coincident with the ring of enhanced values of Φ_{DP}. It is also evident that the ring with enhanced differential phases is surrounded mostly by regions with same phases, i.e., the differential phase below and above the bright band frequently has same values. Thus, there is no significant change in the propagation part of the differential phase. That suggests that the backscatter differential phase can be substantial in the melting layer.

Fig. 2 depicts a part of the range profile of the differential phase at azimuth 300° averaged over 5 successive radials. The rate of antenna rotation was low and 5 consecutive radials comprised a 1° sector. The system differential phase is 18.5° and is shown with the dashed horizontal line. Measured Φ_{DP} oscillates around the system phase at distances shorter than about 39 km, i.e., below the melting layer. In the melting layer, the differential phase experiences strong fluctuations with apparent positive excursion. Above the layer, Φ_{DP} is 1° to 1.5° higher than the system phase. This increase is attributed to propagation differential phase within the melting layer. Analyzing range profiles similar to Fig. 2 we found out that the magnitude of the Φ_{DP} "bump" within the melting layer usually varies between 3° to 7°. We emphasize two main features of the data: **1)** small differential phase 1° to 1.5° due to propagation and consequently small values of the specific differential phase, K_{dp}, and **2)** positive bump of Φ_{DP} up to 7° with the mean value of 4°.

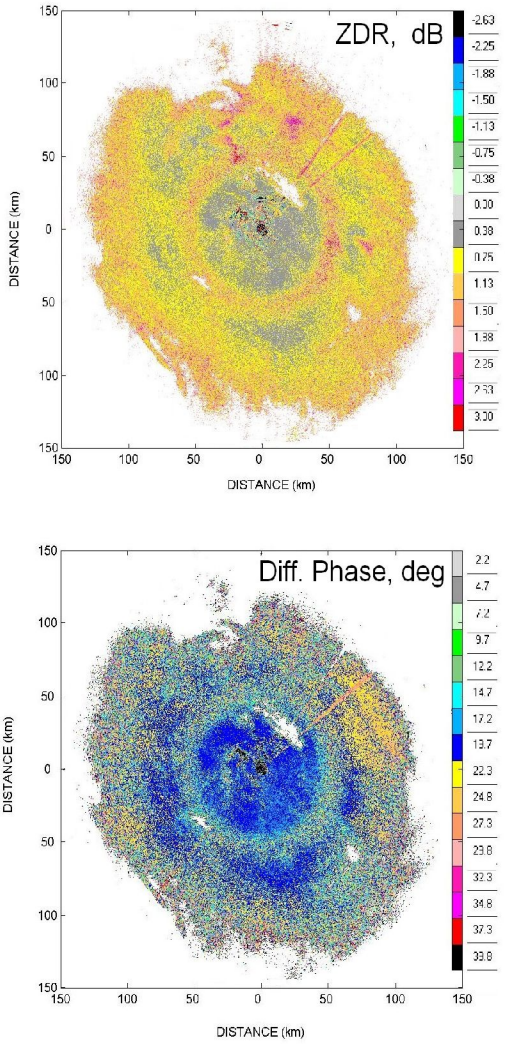

Fig. 1. PPI cross sections of differential reflectivity (top) and differential phase (bottom) recorded with the WSR-88D KOUN radar on February 12, 2005 at 16:49. The antenna elevation is 2.7º.

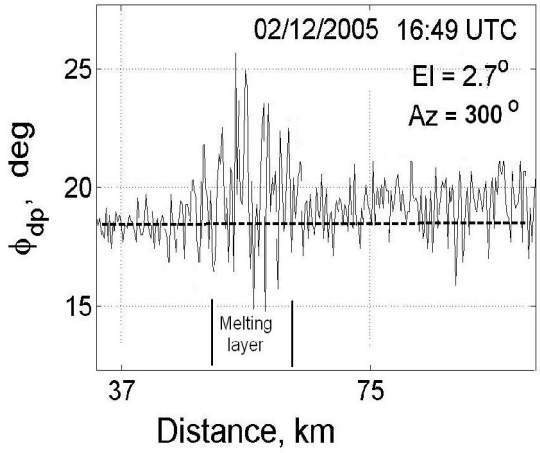

Fig.2. Range profile of the differential phase, φ_{dp}, at azimuth 300º for the field in Fig.1. Data have been obtained with 128 radar samples. The system differential phase is shown with the dash line.

To interpret the data, we consider the resonance and nonuniform beam filling effects mentioned in the introduction. In the absence of backscatter differential phase δ, the nonuniform beam filling produces significant bump in the radial profile of Φ_{DP} only if K_{DP} within the melting layer is sufficiently large and / or the Φ_{DP} difference between two adjacent elevations is big (Ryzhkov and Zrnic 1998). Neither of two is present for the observed data, therefore, we believe that the δ factor should be involved.

Next we consider resonance effects for oblate particles with sizes larger than 10 mm. The effect for water spheroids is demonstrated in Fig.3 with the blue line. The ratio of the major, *a*, and minor, *b*, axes of the spheroid is 1.25 which is close to oblateness of large raindrops. At diameters around 11 mm, δ is negative and changes quickly to large positive values for 13…15 mm particles. The curves have been obtained with the T-matrix code developed by Mischenko et al. 2002. This effect takes place for pure water spheroids with large dielectric permittivity ε. Permittivity of ice is significantly smaller and one can expect diminishing resonance effects for wet snowflakes that can be represented as a mixture of ice and water.

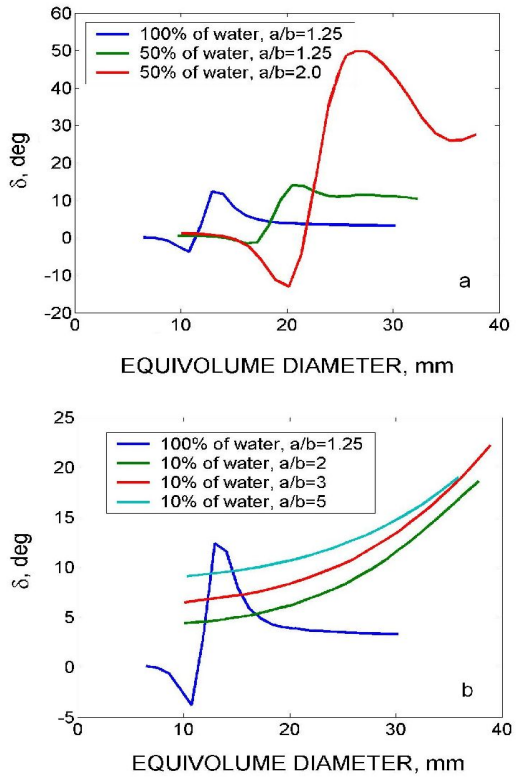

Fig.3. Backscatter differential phase δ for large water spheroids with a/b=1.25 and 50% water content (a), and 10% water content (b). In the bottom figure, δ for water spheroids with a/b=1.25 is shown for reference. Radar wavelength is 11 cm.

Snow particles in the melting layer have large variations of densities from 0.01 to 0.5 g m^{-3} (Magano and Nakamura 1965, Hobbs et al. 1974, Klaassen 1988, Fabry and Szyrmer 1999). Analyzing reflectivities and the terminal velocities of snowflakes in the bright bands, Fabry and Szyrmer 1999 have concluded that the following relation of Mitchel et al. 1990 describes the radar data the best: $\rho_s = 0.015 / D_s$, where ρ_s is the snowflakes' density in g cm^{-3}, D_s is the diameter of the snowflake in cm. Such low densities are associated with small ε so dry, centimeter-size snowflakes cannot have substantial δ caused by the resonance effect. Snowflakes become spongy during melting. Wet spongy snowflakes with large sizes can produce appreciable δ. In Fig. 3a, values of δ are shown for 50% water content. Comparing the blue and green curves we conclude that the decrease of water content shifts the resonance peaks to bigger sizes and makes the negative δ shallower. Comparing the green and red curves we can conclude that for given water content, more oblate particles have more pronounced resonant peaks. The increase of oblateness shifts the positive peaks to the region of very large sizes.

Fig 3b depicts δ for 10% water content. Comparing the blue curve with the rest ones we can conclude that the curves do not look like the Mie resonance dependences. Small water content makes the particles optically "soft" and overall increase of δ is not due to the resonance effect but can be described in terms of Rayleigh scattering (as will be shown in section 4). It is important to note that small particles have rather big positive δ. The positive δ in Fig. 3b could explain the positive bias of the differential phase in the melting layer if nonspherical particles exist in the layer. In the next section, we briefly describe microphysical habits of nonspherical particles within the melting layer reported in the literature.

3. Nonspherical particles in the melting layer

It was shown in the previous section that nonspherical particles consisting of ice and water with oblateness 3…5 can produce appreciable positive backscatter differential phase. The question is whether such particles exist in the melting layer. High ZDR and LDR routinely observed in the melting layer prove that the hydrometeors are essentially nonspherical there.

Direct measurements of hydrometeors in the melting layer are very scarce. Willis and Heymsfield (1989) have presented data on concentration of particles with diameters larger than 1.9 mm which show the presence of large nonspherical hydrometeors. But no data is available on the oblateness of the particles. For ice clouds, Korolev and Isaac (2003) have presented images of ice cloud particles that show high nonsphericity for particles with diameters up to 0.5 mm. Their results show an increase of mean oblateness to 1.3 … 1.4 (in terms of a/b) for particles with diameters close to 1 mm. From their data for diameters larger than 1.2 mm and temperature interval -5 to 0º C, one can see that the mean oblateness is close to 2 with many nonspherical particles with oblateness up to 5. Pictures of highly nonspherical melting snowflakes have been presented by Fijiyoshi (1986). Studying of optical properties of ice clouds Liou and Takano (1994) considered large ice dendrites with oblateness up to 20. Heymsfield and Miloshevich 2003 and Liu 2004 have reported on thickness of cloud ice rosettes and dendrites with diameters 1 to 5 mm and oblateness from 5 to 20. Russchenberg and Ligthart (1996) have shown that good agreement with radar data can be achieved if

snowflakes' oblateness is near 3 at the beginning of melting. During melting the oblateness decreases to values near 1 for water droplets.

The cited literature sources allow for concluding that oblateness of large snowflakes in the melting layer can be 3…5 and probably can exceed these values for large dendrites. Cloud particles with sizes less than 5 mm can have oblateness of 3 ..5 and more. In the next section, we consider backscatter differential phases for nonspherical particles with oblateness up to 20, and our focus is on particles with oblateness 3…5.

4. Backscatter differential phase for the Rayleigh scatteres

Above the bright band the scatterers are ice particles and below the band they are droplets. Inside the band, wet snowflakes coexist with dry ice particles and droplets. The relative number of each type of the particles depends on the proximity to the top or bottom of the melting layer. Most popular radar model for melting snowflakes is a "spongy" particle with almost homogeneous mixture of ice and water (Russchenberg and Ligthart 1996, Fabry and Szyrmer 1999, Szyrmer and Zawadzki 1999, D'Amico et al. 1998). We present our results on backscatter differential phase for spongy snowflakes in subsection *b* below. We also consider δ for a melting particle modeled as an oblate ice spheroid covered with a water film (subsection *c*). The Rayleigh approximation is used in this section as appropriate for S band.

a) Homogeneous particles

Begin with homogeneous particles and assume that in the mean, snowflakes can be modeled as oblate spheroids. We consider here a particle with axes *a* and *b* in horizontal and vertical directions ($a > b$). Let the particle be horizontally oriented, i.e., the canting angle is zero. The elements of amplitude scattering matrix for horizontally, S_{hh}, and vertically, S_{vv}, polarizations can be represented as (e.g., Bringi and Chandrasekar 2001, section 2.3)

$$S_{hh} = -\frac{k}{4\pi\varepsilon_o}\alpha_h, \qquad S_{vv} = -\frac{k}{4\pi\varepsilon_o}\alpha_v, \quad (1)$$

where k is the wavenumber,

$$\alpha_h = \frac{4}{3}\pi a^2 b \frac{\varepsilon_1 - \varepsilon_0}{\varepsilon_0 + L_h(\varepsilon_1 - \varepsilon_0)}, \quad (2a)$$

$$L_h = 0.5 f^{-2}\left(\frac{1-f^2}{f^2}\right)^{1/2}\left[\frac{\pi}{2} - a\tan\left(\frac{1-f^2}{f^2}\right)^{1/2}\right] - 0.5\left(\frac{1-f^2}{f^2}\right), \quad (2b)$$

$$f^2 = 1 - b^2/a^2, \quad (2c)$$

and ε_0 , ε_1 are permittivity of air and the particle correspondingly. For vertically polarized wave, α_v has the same form as (2a) with $L_v = 1 - 2L_h$. S_{hh} and S_{vv} are equal for a spherical particle so there is no backscatter differential phase in that case. For spheroids, S_{hh} and S_{vv} differ and the backscatter differential phase δ is

$$\delta = \arg(S_{hh}) - \arg(S_{vv}). \quad (3)$$

It is evident that the differential phase is a function of permittivity and the shape. The imaginary part of permittivity of ice is small therefore δ is small for ice particles with any oblateness. At S band, for water at temperature 0° C, ε_1 = 79.7 - 25.2i (Meneghini and Kozu, 1990) with significant imaginary part so that a considerable δ can be expected. In Fig. 4, δ for water and ice particles are shown as functions of oblateness. One can see that δ increases with the oblateness and for water drops with oblateness 20 it reaches 4°. Such oblateness is not realistic for water droplets.

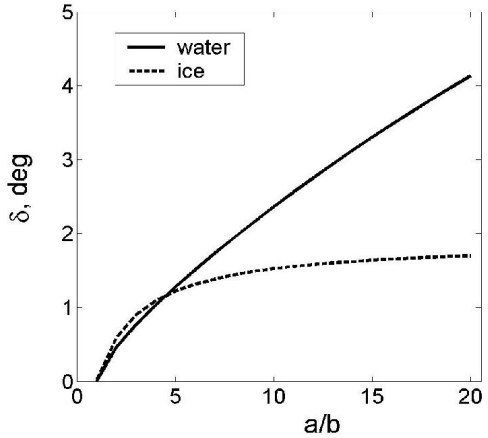

Fig.4. Backscatter differential phase δ for oblate water and ice particles.

b) Spongy spheroids

Next we model a particle as a homogeneous mixture of ice and water. For a rigid particle with small permittivity and imbedded water, Meneghini and Liao (1996) have concluded that, the Maxwell-Garnet formula with water as the matrix gives better results than water as inclusion. So we write for the effective dielectric constant for a wet snowflake

$$\varepsilon_{eff} = \varepsilon_w \frac{1+2Ec}{1-Ec}, \qquad (4)$$

$$E = \frac{\varepsilon_i - \varepsilon_w}{\varepsilon_i + 2\varepsilon_w}, \qquad (5)$$

where c is the volume fraction of ice ($0 \le c \le 1$), ε_w and ε_i permittivity of water and ice. Because $\varepsilon_w >> \varepsilon_i$ we neglect ε_i in (5) and get $E \approx -0.5$. Substitution of the latter into (4) yields

$$\varepsilon_{eff} \approx \varepsilon_w \frac{1-c}{1+0.5c}, \qquad (6)$$

One can see from (8) that the effective dielectric constant can be a small part of the dielectric constant of water at $c \to 1$, i.e., when melting process begins. Fig. 5 shows δ for wet snowflakes. It is seen that δ can exceed 10° for oblateness 5 and for small water contents.

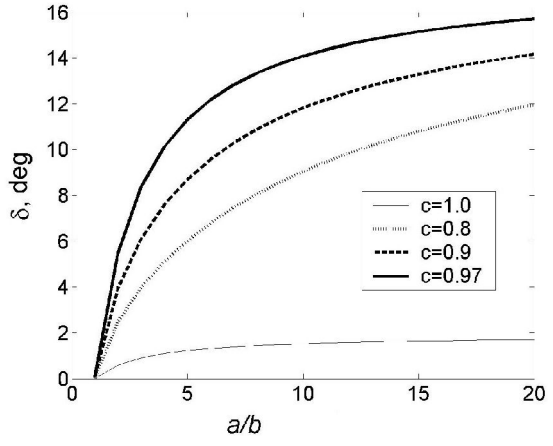

Fig. 5. Backscatter differential phase δ for wet spongy snowflakes for different ice volume fractions c.

c) ***Oblate ice particles covered with water films***

Consider also an oblate ice core coated with a thin water film. Such a model can be applied for melting snowflakes (Fujyoshi 1986, Fabry and Szyrmer 1999). Let a_1 and b_1 be the axes of the ice core and a_2 and b_2 be the axes of the whole particle. For a coated spheroid, relation (2a) can be written as (Bohren and Huffman 1983, section 5.4)

$$\alpha_h = \frac{4}{3}\pi a_2^2 b_2 \frac{(\varepsilon_w - \varepsilon_0)\{\varepsilon_w + A\} + F\varepsilon}{\{\varepsilon_w + A\}B + G}, \qquad (7)$$

where

$$A = (\varepsilon_i - \varepsilon_w)[L_h^{(1)} - FL_h^{(2)}],$$
$$B = \varepsilon_0 + (\varepsilon_w - \varepsilon_0)L_h^{(2)},$$
$$G = FL_h^{(2)}\varepsilon_w(\varepsilon_i - \varepsilon_w),$$
$$F = a_1^2 b_1 / a_2^2 b_2,$$

$L_h^{(1)}, L_h^{(2)}$ are factors (2b) for the inner and outer spheroids. In Fig. 6, the phase δ is shown as a function of oblateness for different thickness of the water film. The thickness is calculated relative to the radius of the equivolume water sphere. Differential phase δ increases with the thickness to the relative thickness of about 0.02 and then drops down to the water value. It is seen from the figure that the backscatter differential phase is about 3° for particles with oblateness 5.

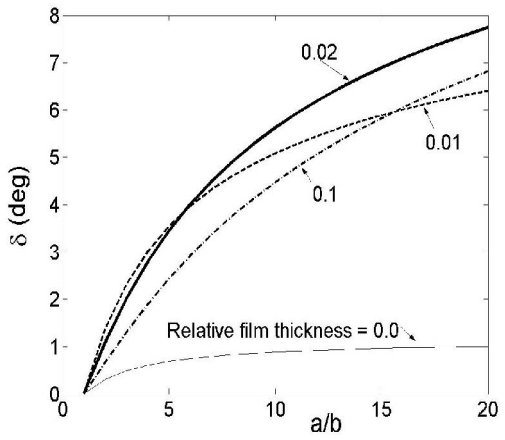

Fig. 6. Backscatter differential phase δ for oblate ice spheroids coated with a water film. The thickness of the film is shown relative to the radius of the equivolume sphere.

5. Discussion

In the melting layers of analyzed widespread winter precipitation in Oklahoma, differential phase exhibits a positive "bump" as large as 7º with an average magnitude of 4º. The propagation component of Φ_{DP} through melting layer is only 1.5 – 2.0º. We tend to think that the positive deviation of 2º to 5º is due to backscatter differential phase δ.

There are two possible explanations for tangible δ known from the literature: first – large water-coated or spongy snowflakes with oblateness that is not much different from the one of large raindrops. Second – nonuniform beam filling. Both explanations may not be reasonable for the case illustrated in the paper because (a) moderately oblate snowflakes have to be quite large to produce noticeable δ and such large spongy snowflakes should have high reflectivity which is not the case; (b) deviations of Φ_{DP} due to nonuniform beam filling cannot exceed the Φ_{DP} difference between adjacent rays with different elevations at the same ranges. Since the propagation differential phase is small for a given ray (less than 2º) then this explanation is also disputable.

The resonance effect for water spheroids that causes negative and positive δ, is suppressed in wet snowflakes with water contents less than 40%. This effect can cause large positive and negative δ for melting snowflakes with sizes more than 2 mm and oblateness exceeding 2. The literature sources allow assuming that oblateness of snowflakes can exceed 2 and ice particles just above the melting layer can have oblateness of 5 and higher.

At the beginning of melting, effective permittivity of the wet snowflake can be significantly lower than permittivity of water. The particle is optically "soft" and the Rayleigh approximation can be used in the calculations of δ. Soft Rayleigh particles have positive δ only. Oblate spongy particles can cause δ about +10º if oblateness is around 5. Water content in such particles can be 3 …5%. Calculated backscatter phases could contribute to the observed positive biases of the differential phases in the melting layer. It should be noted that the effect of nonuniform beam filling can be enhanced by δ and there might be a combination of the effect and δ.

We speculate on three possible mechanisms for the positive differential phases in the melting layer. Each mechanism could play a role at different stages of melting. We believe that comparisons of the differential phases at different wavelengths (S, and/or C, X bands) will shed more light on the observed effect because all three mechanisms are quite sensitive to the radar wavelength.

Acknowledgments

This paper was prepared with funding provided by NOAA/Office of Oceanic and Atmospheric Research under NOAA-University of Oklahoma Cooperative Agreement #NA17RJ1227, U.S. Department of Commerce. The statements, findings, conclusions, and recommendations are those of the authors and do not necessarily reflect the views of NOAA or the U.S. Department of Commerce.

References

Balakrishnan, N., and D.S. Zrnic, 1990: Use of polarization to characterize precipitation and discriminate large hail. *J. Atmos. Sci.*, **47**, 1525-1540.

Bohren C.F., and D.R. Huffman, 1983: *Absorption and scattering of light by small particles.* New York, John Wiley&Sons.

Bringi, V. N. and V. Chandrasekar, 2001: *Polarimetric Doppler Weather Radar.Principles and Applications.* Cambridge University Press. 636 pp.

D'Amico M. M. G., A. R. Holt, and C. Capsoni, 1998: An anisotropic model of the melting layer. *Radio Sci.*, **33**, 535-552.

Doviak, R. J. and D. S. Zrnic, 1993: *Doppler radar and weather observations*, 2nd ed., Academic Press, 562 pp.

Fabry, F., and W. Szyrmer, 1999: Modeling of the melting layer. Part II: electromagnetics. *J. Atmos. Sci.*, **56**, 3593-3600.

Fujyoshi Y., 1986: Melting snowflakes. *J. Atmos. Sci.*, **43**, 307-311.

Heymsfield, A. J., and L.M. Miloshevich, 2003: Parameterization of the cross-sectional area and extinction of cirrus and stratiform ice cloud particles. *J. Atmos. Sci.*, **60**, 936-956.

Klaassen, W., 1988: Radar observation and simulation of the melting layer of precipitation. *J. Atmos. Sci.*, 45, 3741-3753.

Liou, K.N., and Y. Takano, 1994: Light scattered by non-spherical particles: Remote sensimg and climate applications: *Atmos. Res.*, 31, 271-298.

Liu G., 2004: Approximation of single scattering properties of ice and snow particles for high microwave frequencies. *J. Atmos. Sci.*, **61**, 2441-2456.

Meneghini, R., and T. Kozu, 1990: *Spaceborn Weather Radar*. Boston, MA, Artech House.

Meneghini, R., and L. Liao, 1996: Comparison of cross sections for melting hydrometeors as derived from dielectric mixing formulas and a numerical method. *J. Applied Meteor.*, **35**, 1658-1670.

Mitchel, D. L., R. Zhang, and R.L. Pitter, 1990: Mass-dimensional relationships for ice particles and the influence of riming on snowfall rates. *J. Applied Meteor.*, **29**, 153-163.

Mischenko M. I., L.D. Travis, and A.A. Lacis, 2002: *Scattering, Absorbtion, and Emission of Light by Small Particles*. Cambridge University Press, 228 pp.

Russchenberg H. W..J., and L. P. Ligthart, 1996: Backscattering by and propagation through the melting layer of precipitation: a new polarimetric model. IEEE Trans**., GRS-34**, 3-14.

Ryzhkov A.V., and D.S. Zrnic, 1998: Beamwidth effects on the differential phase measurements of rain, *J. Atmos.Oceanic Technol.*, **15,** 624–634**.**

Szyrmer, W., and I. Zawadzki, 1999: Modeling of the melting layer. Part I: Dynamics and microphysics. *J. Atmos. Sci.*, **56**, 3573-3592.

Zrnic D.S., N. Balakrishnan, C.L. Ziegler, V.N. Bringi, K. Aydin, T. Matejka, 1993: Polarimetric signatures in the stritiform region of a mesoscale convective system. *J. Applied Meteor.,* **32**, 678 – 693.